Maneuverability and Envelope Protection in the Prevention of Aircraft Loss of Control

Robert C. Allen Harry G. Kwatny
Department of Mechanical Engineering and Mechanics
Drexel University
Philadelphia, PA 19104, USA
e-mail: rca28@drexel.edu, hkwatny@coe.drexel.edu

***Abstract*—Loss-of-Control (LOC) is a major factor in fatal aircraft accidents. Although definitions of LOC remain vague in analytical terms, it is generally associated with a diminished capability of the pilot maneuver the aircraft - whether due to impairment of the aircraft or its entry into an unfavorable flight regime. Maneuver performance is usually assessed by evaluating an aircraft's ability to transition between desired steady state conditions such as wings level climb, descent, or coordinated turns. We show that even when a sufficient set of steady motions exist, the ability to regulate around them or transition between them can be difficult and non-intuitive, particularly for impaired aircraft. We examine the impact of control constraints, including those induced by actuator impairment, on the ability to prevent envelope departure and to maneuver within it. Safe set theory can be used as a basis for design of envelope protection systems. Higher dimensional safe sets are difficult to compute and visualize. For the full conventional longitudinal dynamics we present an analytic solution to a Hamiltonian which specifies the optimal safety critical control. We then use this expression in a numerical level set framework to compute four dimensional safe sets. Examples are provided using NASA's Generic Transport Model (GTM).**

I. Introduction

Loss-of-Control (LOC) is a principle factor in commercial aircraft accidents, (1). Although LOC has not yet been precisely defined in analytical terms it is associated with a pilot's inability to regulate key aircraft variables, (2; 3). Recent research connects LOC with in-flight bifurcation phenomenon – ordinarily associated with stall in aircraft, (4; 5). When a vehicle maneuvers near those critical points, it loses the ability to be regulated due to the occurrence of structurally unstable zero dynamics, (6). Furthermore, the ability to maneuver an aircraft within a *safe* envelope can be difficult because of variation of the trim point structure within it – particularly when the aircraft is impaired, (5). The trim point structure is organized by bifurcation points even though they may lie outside of the safe envelope.

LOC is likely to occur when an aircraft operates in the vicinity of a stall (bifurcation) point or when a maneuver from one steady motion to another requires switching to a different trim branch. In the latter case, stabilization around the new trim point will require a change in piloting strategy thus contributing to confusion, potentially resulting in LOC. Recovery from LOC, requires restoration of the vehicle to a suitable trim point around which it can be satisfactorily regulated.

Ordinarily a flight envelope can be considered a convex polyhedral set, not necessarily bounded, in the state space. Ensuring that an aircraft remains within its flight envelope is called *envelope protection*. Envelope protection is generally the responsibility of the pilot although there is an increasing interest in and use of automatic protection systems (7; 8; 9). We consider the control issues associated with preventing departure from the flight envelope. To do so, we use the notion of a *safe set* (10) or *viable set* (11). The idea of a safe set derives from a decades old control problem in which the plant controls are restricted to a bounded set $\mathcal{U}$ and it is desired to keep the system state within a convex, not necessarily bounded, subset $\mathcal{C}$ of the state space. (12) studied the question: under what conditions does there exist for each initial state in $\mathcal{C}$ an admissible control producing a trajectory that remains in $\mathcal{C}$ for all $t > 0$? When $\mathcal{C}$ does not have this property we try to identify the safe set, $\mathcal{S}$, that is, the largest subset of $\mathcal{C}$ that does. Clearly, if we wish the aircraft to remain in $\mathcal{C}$, we must ensure that it remains in $\mathcal{S}$.

We would also like to know how the aircraft can maneuver within $\mathcal{S}$. Controlled flight requires the existence of a suitable set of steady motions and the ability to smoothly transition between them. This means that we need to understand the equilibrium point structure within $\mathcal{S}$ and identify any impediments to regulating around them or steering from one to another.

Ordinarily, if an aircraft is impaired we expect that the safe set will shrink. We will show that the equilibrium point structure within the reduced safe set changes as well and the ability to maneuver is significantly diminished. Furthermore, control strategies required to execute transition maneuvers and to regulate around steady motions may be complex and non-intuitive. We suggest this as another mechanism of LOC.

II. GTM Model

Examples in this paper are based on NASA's Generic Transport Model (GTM). In this paper we extend the phugoid analysis presented in, (4; 5), to the full longitudinal dynamics and add additional higher order aerodynamic terms. The resulting model has four dimensions and presents more challenges for both the visualization and computation of trim states and safe sets.

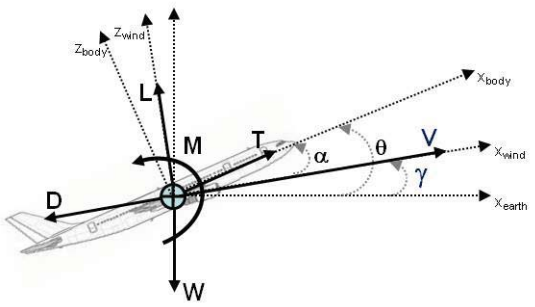

Fig. 1. Free Body Diagram of 3-DOF Longitudinal Model

A. GTM Longitudinal Dynamics

The longitudinal dynamics of a rigid aircraft shown in Figure 1 can be written in path coordinates:

$$\begin{aligned}
\dot{V} &= \tfrac{1}{m}\left(T\cos\alpha - \tfrac{1}{2}\rho V^2 S C_D\left(\alpha,\delta_e,q\right) - mg\sin\gamma\right)\\
\dot{\gamma} &= \tfrac{1}{mV}\left(T\sin\alpha + \tfrac{1}{2}\rho V^2 S C_L\left(\alpha,\delta_e,q\right) - mg\cos\gamma\right)\\
\dot{q} &= \tfrac{M}{I_y},\\
\dot{\alpha} &= q - \dot{\gamma}
\end{aligned} \tag{1}$$

where

$$\begin{aligned}
M = \tfrac{1}{2}\rho V^2 S\bar{c} C_M\left(\alpha,\delta_e,q\right) + \tfrac{1}{2}\rho V^2 S\bar{c} C_Z\left(\alpha,\delta_e,q\right)\\
\left(x_{cgref} - x_{cg}\right) - mgx_{cg}\cos\left(\theta\right) + l_t T
\end{aligned}$$

and $\theta = \alpha + \gamma$. To illustrate safe set computations in this paper we assume that we are given an operating envelope

$$\begin{aligned}
\mathcal{C} = \{(V,\gamma,q,\alpha) | 90 \le V \le 240, -22 \le \gamma \le 22,\\
-10 \le q \le 10, -6 \le \alpha \le 22\}
\end{aligned} \tag{2}$$

and a control restraint set specified by

$$\mathcal{U} = \{(T,\delta_e)\,|0 \le T \le 30, -40 \le \delta_e \le 20\,\} \tag{3}$$

III. Maneuverability and the Trim Set

A. Trim Behavior of the Longitudinal Dynamics

For commercial aircraft one of the most basic and important steady motion is straight, wings level, climbing and descending flight. We will examine this steady motion for a specified speed and flight path angle (V,γ). An equilibrium (or trim) condition exists when all four of the state derivatives ($\dot{V},\dot{\gamma},\dot{q},\dot{\alpha}$) in (1) are zero. For straight, wings level flight both $q = 0$ and $\dot{\gamma} = 0$, so it follows that $\dot{\alpha} = 0$ and the governing equations for an equilibrium point reduce to three equations and three unknowns, T, δ_e, and α. Let the solutions to these trim equations be denoted by T^*, ${\delta_e}^*$, and α^*.

The trim equations can be solved numerically by defining a scalar cost function which is sum of the squares of the derivatives ($\dot{V},\dot{\gamma},\dot{\alpha}$). To then account for the limits on the control variables a matlab algorithm by (13) was utilized. Results of these computations for steady motion are shown in Figure 2. Starting at the black dots as airspeed drops the trim points follow the lower branch of the thrust and angle of attack curves and the upper branch of the elevator curve until the bifurcation (stall) point is reached (black triangles). This solid line represent the 'normal' trim points, but there is an additional branch (dashed lines) comprised of viable trim points so long as the thrust and elevator are within bounds. This observation can be important, as we will see below. We might refer to these as *high angle of attack* trim points. The high angle of attack trim points are characterized by low speeds, high values of thrust, and large negative elevator commands (nose up). They exist at lower speeds where there is less dynamic pressure which means greater angles of attack are necessary to generate sufficient lift, resulting in a sizeable induced drag, which must be balanced by thrust. Another key point of the results is that the trend of the equilibrium thrust curves suggest that negative values will be required at some airspeeds with flight path angles less than -3 deg, making those trim states not viable.

An essential point is that the control behaviors around trim points on the two branches are considerably different so that a strategy to regulate around a point on one branch will fail if applied to one on the other branch. The theoretical basis for this is established in (6; 14; 15; 16). We will give a simple example for these results. Consider the two trim points at V=90 fps and $\gamma = 0\,\mathrm{deg}$: the *normal trim point* solution $T^* = 7.628525$ lbf, ${\delta_e}^* = -8.498114$ deg, $\alpha^* = 11.90566$ deg, and the *high angle of attack trim point* solution $T^* = 20.957574$ lbf, ${\delta_e}^* = -17.451446$ deg, $\alpha^* = 18.959770$ deg. The eigenvalues of the linearized dynamics at each of these trim points are, first for the normal trim:

$$eig(A) = \left\{ \begin{array}{c} -0.425 \pm 4.93i \\ -0.0783 \pm 0.534i \end{array} \right\}$$

and for the high angle of attack trim:

$$eig(A) = \left\{ \begin{array}{c} 0.553 \pm 6.39i \\ -0.158 \pm 0.448i \end{array} \right\}$$

Inspection of the eigenvalues for the normal angle of attack shows that for the phugoid mode, ($\zeta = .145, \omega_n = 0.539$) and for the short period mode ($\zeta = 0.086, \omega_n = 4.95$). For the high angle of attack trim the phugoid mode is ($\zeta = 0.33, \omega_n = 0.475$) the short period mode is *unstable*. Clearly regulation around upper branch trim points will require a different strategy due to the instability of the short period mode.

This behavior is organized by a bifurcation point that separates the two branches. As shown in (5), a static bifurcation point occurs when a degeneracy occurs in the zero dynamics of

$$\begin{aligned}
\dot{x} &= f(x,u,\mu)\\
z &= h(x,\mu)
\end{aligned} \tag{4}$$

where $x \in R^n$ are the states, $u \in R^p$ are the control inputs, $z \in R^r$ are the regulated variables and $\mu \in R$ is any parameter. The values for the bifurcation points in Figure 2 are shown in Table I for regulation of speed and flight path angle (V,γ). Examination of the linearized zero dynamics at each of these

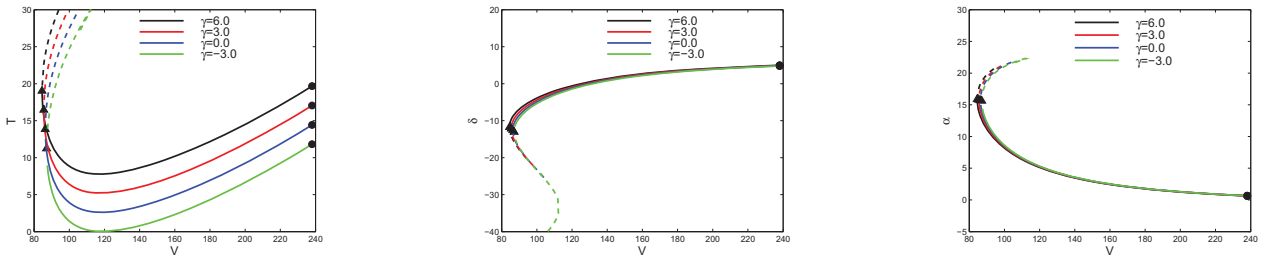

(a) Thrust (b) Elevator Position (c) Angle of Attack

Fig. 2. Trim values for thrust, elevator and angle of attack as a function of airspeed, V, are shown for various flight path angles $\gamma = 6, 3, 0, -3$. High angle of attack trim states are depicted by dashed lines and are characterized by low speeds, high values of thrust, and large negative elevator commands (nose up). There are 1, 2, and in some cases 3 admissible control pairs to each viable trim point.

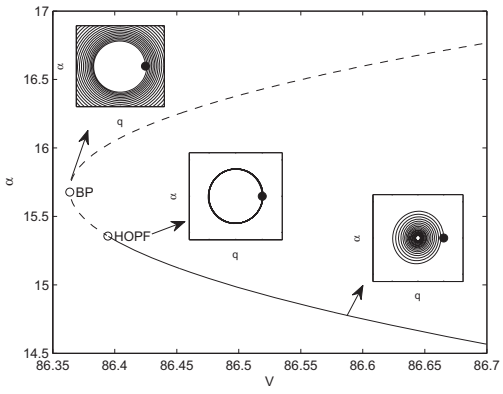

Fig. 3. Closeup of angle of attack bifurcation curve of Figure 2 for $\gamma = 0$ shows that a portion of the normal angle of attack is also unstable up to the speed where a Hopf bifurcation is encountered. The insets show the oscillatory behavior of the $\alpha - q$ dynamics at various points on the bifurcation curve for a small perturbation in pitch rate, q.

bifurcation points shows that a degeneracy occurs in the form of two transmission zeros at the origin. Figure 3 shows a close up of the bifurcation dynamics at the bifurcation point for $\gamma = 0$. Note that the normal angle of attack branch is also unstable in the vicinity of the bifurcation point, and as airspeed increases, a Hopf bifurcation occurs as the complex conjugates of the short period eigenvalues cross the imaginary axis and become stable.

TABLE I
BIFURCATION POINTS

γ	V	T^*	$\delta_e{}^*$	α^*
6	84.493095	18.982517	-11.706503	15.843524
3	85.494013	16.428146	-12.160762	15.759063
0	86.363679	13.828949	-12.599274	15.677520
-3	87.103862	11.192067	-13.025417	15.598298

Note that for each flight path angle the thrust required for steady flight has a region to the left of the minimum value along the lower trim branch where increasing levels of thrust are required for equilibrium conditions at lower airspeeds. This can be loosely referred to as the power curve though it is not the same as the power-required curve, (17), since engine characteristics are not included. The region the the left of the minimum of the power-required curve is what pilots refer to as flying on the *backside of the power curve*. We have shown that an additional trim branch also exists in this regime where increasing thrust increases airspeed, however regulation around these points could be difficult and non-intuitive due to the instability of the short period mode.

B. Trim Points

With bounded controls there are four possible outcomes for each possible trim point; (1) it is not attainable; (2) it is only attainable at a high angle of attack; (3) it is only attainable at a normal angle of attack; and (4) it is attainable at both a high and normal angle of attack. For all viable trim points we have shown that there are 1, 2, and in some cases 3 admissible control pairs.

Attainable (V,γ) trim points are summarized in Figure 4 on a discrete 2D grid spanning the flight envelope. Transition from normal to high angle of attack trim (or vis-versa) could be difficult because of the short period mode instability. The pilot (or auto-pilot) needs to recognize the need to change control strategy accordingly. Of course, this picture is altered in significant ways if flaps, spoilers even landing gear are deployed.

In the restricted elevator case shown in Figure 4 the elevator range of motion is limited in the positive direction to 3 degrees. This severely limits the set of normal flight trim points. For a jammed elevator the set of viable trim points reduces to a curve where only normal angle of attack trim points exist.

IV. SAFE SET FOR LONGITUDINAL DYNAMICS

There are two fundamental issues that need to be addressed: Is it possible to remain within a specified subset of the state space? If so, what control actions are required to insure the aircraft remains within it? These questions have been examined in the literature, e.g., (18; 11; 10). Suppose that $\mathcal{C}$ is defined by

$$\mathcal{C} = \{x \in R^n \,|\, l(x) > 0\} \tag{5}$$

where $l : R^n \to R$ is continuous. The boundary of $\mathcal{C}$ is the zero level set of l, i.e., $\partial\mathcal{C} = \{x \in R^n \,|\, l(x) = 0\}$. The safe set is defined as the largest positively control-invariant set contained in $\mathcal{C}$. Several investigators have considered the computation of the safe set, the most compelling of which involve solving the

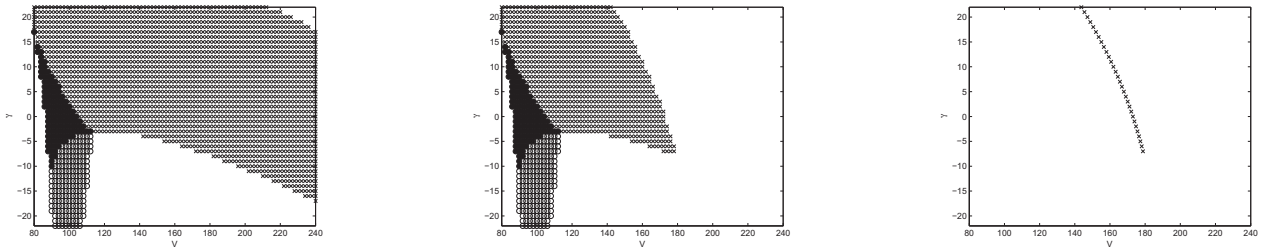

(a) Unimpaired (b) Restricted Elevator (c) Jammed Elevator

Fig. 4. Trim set (V, γ) with various levels of elevator impairment. The figure on the left shows attainable trim set for the unimpaired aircraft in which case the elevator position ranges from -40 deg to +20 deg. In the center figure, the elevator motion is restricted in the positive direction to + 3 deg. On the right is the trim set for the aircraft with elevator jammed at 3 deg. An "x" denotes existence of only a normal angle of attack trim, an "o" denotes existence of only a high angle of attack trim and a filled circle indicates the both trim states are attainable.

Hamilton-Jacobi equation. In (11) it is shown that if $V(x,t)$ is a viscosity (or, weak) solution of the terminal value problem

$$\frac{\partial V}{\partial t} + \min\left\{0, \sup_{u\in U} \frac{\partial V}{\partial x} f(x,u)\right\} = 0, \quad V(x,T) = l(x) \tag{6}$$

then

$$\mathcal{S}(t,\mathcal{C}) = \{x \in R^n \,|V(x,t) > 0\} \tag{7}$$

$V(x,t)$ is the unique, bounded and uniformly continuous solution of (6) and is in fact the 'cost-to-go' associated with an optimal control problem in which the goal is to choose $u(t)$ so as to maximize the minimum value of $l(x(t))$. Define the Hamiltonian of (6) to be

$$H(p,x) = \max_{u\in U} p^T f(x,u) \tag{8}$$

Notice that the control obtained in computing the Hamiltonian (8) ensures that when applied to each state along any trajectory initially inside of $\mathcal{S}$ the resulting trajectory will remain in $\mathcal{S}$. It follows that this control should be applied for states on its boundary to ensure that the trajectory does not leave $\mathcal{S}$.

Obtaining an analytic solutions to (6) is virtually impossible for realistic models of dimension higher that two. To overcome this limitation, numerical level set methods are typically employed. The four dimensional results obtained in this paper are obtained using the numerical level set framework developed by (19) which is based on algorithms in (20).

One of the great challenges of utilizing numerical level set methods is obtaining a computationally efficient analytic solution for the Hamiltonian of (8). Let the solution to (8) be $u^* = \{T^*, \delta_e^*\}$ for a specified location in the state space, x, and gradient, $\frac{\partial V}{\partial x}$. The remainder of this section will present necessary background material for analytic expressions of the optimal thrust and elevator.

Substituting the longitudinal dynamics (1) into (8) results in

$$H(x,p) = \max_{u\in\mathcal{U}} \mathcal{H}(x,p,u)$$

$$\mathcal{H}(x,p,u) = \left(p_1\dot{V} + p_2\dot{\gamma} + p_3\dot{q} + p_4\dot{\alpha}\right)$$

Expressing the aerodynamic coefficients in Hamiltonian in terms of state and control variables and noting there are no terms involving cross products of the control variables the Hamiltonian can be simplified to the sum of two single variable optimization problems and a constant,

$$\mathcal{H}(x,p,u) = \mathcal{H}_T(x,p,T) + \mathcal{H}_{\delta_e}(x,p,\delta_e) + H_0(x,p) \tag{9}$$

Thus,

$$H(x,p) = H_T(x,p) + H_{\delta_e}(x,p) + H_0(x,p)$$

where

$$H_T(x,p) = \max_{T\in\mathcal{U}_T} \mathcal{H}_T,\ H_{\delta_e}(x,p) = \max_{\delta_e\in\mathcal{U}_{\delta_e}} \mathcal{H}_{\delta_e}$$

$H_0(x,p))$ is a constant and needs to be evaluated only once. $\mathcal{H}_T(x,p,T)$ is linear in T, the optimal thrust will exist be one of the extreme points of $\mathcal{U}_T$. $H_{\delta_e}(x,p)$ is a non-linear optimization problem since $\mathcal{H}_{\delta_e}$ is cubic in δ_e. A necessary condition for a maximum to exist on the interior of $\mathcal{U}_{\delta_e}$ is that

$$\frac{\partial \mathcal{H}_{\delta_e}(x,p,\delta_e)}{\partial \delta_e} = 0$$

at a point in the interior. This equation is quadratic in δ_e. The second derivative of the Hamiltonian with respect to δ_e is needed to tell if the stationary point is a local minimum, maximum, or indeterminate.

A. Optimal Safe Set Control

In this section the solution for the optimal thrust, T^*, and elevator, ${\delta_e}^*$, is presented. We will show that the optimal thrust is always at an extrema of the control limits which is typical of solutions to this type of problem. However, for the elevator the solution need not always be at a limit.

1) Optimal Thrust for Hamiltonian.: To keep the aircraft within the flight envelope constraints, the optimal thrust, T^*, will typically assume one of two values $\{T_{\min}, T_{\max}\}$. The only exception is if the constant term is exactly zero then T^* is a set valued quantity and any value of thrust in the interval $[T_{\min}, T_{\max}]$ is a solution. This constant term need only evaluated once, then the optimal thrust and therefore $H(x,p)_T$ can be fully determined.

$$T^* = \left\{ \begin{array}{ll} T_{\min} & if\left(\begin{array}{c} \frac{p_3 l_t}{I_y} + \frac{p_1\cos\alpha}{m} + \frac{p_2\sin\alpha}{mV} \\ -\frac{p_4\sin\alpha}{mV} < 0 \end{array} \right) \\ T_{\max} & \text{otherwise} \end{array} \right\}$$

2) Optimal Elevator for Hamiltonian.: The pseudo code (algorithm) for computing the optimal elevator for the Hamiltonian (8) is given below. The algorithm for computing $\delta_e{}^*$, has four branches: (1) where the elevator is jammed; (2) where both zeros are outside the interval $[\delta_{\min}, \delta_{\max}]$; (3) one and only one zero is in the interval $[\delta_{\min}, \delta_{\max}]$; and (4) both zeros are in the interval $[\delta_{\min}, \delta_{\max}]$. It is important to note that unlike the optimal thrust, the optimal elevator, $\delta_e{}^*$, is not always at the control limits. The optimal elevator may be counterintuitive in some instances. It is shown that $p^T \cdot f(x, \delta_e)$ need only be evaluated for at most four different values of δ_e to obtain $\delta_e{}^*$.

$$
\begin{array}{l}
if\ (\delta_{\min} = \delta_{\max})\ then \\
\quad \delta_e{}^* = \delta_{\min} \\
elseif\ (\delta_{ez1} \notin [\delta_{\min}, \delta_{\max}] \wedge \delta_{ez2} \notin [\delta_{\min}, \delta_{\max}]) \\
\quad \delta_e{}^* = \underset{\{\delta_{\min}, \delta_{\max}\}}{argmax}\ (p^T \cdot f(x, \delta_e)) \\
\\
elseif\ ((\delta_{ez1} \in [\delta_{min}, \delta_{\max}] \oplus \delta_{ez2} \in [\delta_{min}, \delta_{\max}])) \\
\quad if\ \left(\frac{\partial^2 H(x,p)}{\partial {\delta_e}^2}\Big|_{\delta_{interior}} > 0 \right) \\
\quad\quad \delta_e{}^* = \underset{\{\delta_{\min}, \delta_{\max}\}}{argmax}\ (p^T \cdot f(x, \delta_e)) \\
\quad elseif\ \left(\frac{\partial^2 H(x,p)}{\partial {\delta_e}^2}\Big|_{\delta_{interior}} < 0 \right) \\
\quad\quad \delta_e{}^* = \delta_{interior} \\
\quad else \\
\quad\quad \delta_e{}^* = \underset{\{\delta_{interior}, \delta_{\min}, \delta_{\max}\}}{argmax}\ (p^T \cdot f(x, \delta_e)) \\
\\
elseif\ (\delta_{ez1} \in [\delta_{min}, \delta_{\max}] \wedge \delta_{ez2} \in [\delta_{min}, \delta_{\max}]) \\
\quad if\ \left(\frac{\partial^2 H(x,p)}{\partial {\delta_e}^2}\Big|_{\delta_{ez1}} < 0 \right) \\
\quad\quad \delta_e{}^* = \underset{\{\delta_{ez1}, \delta_{\min} \vee \delta_{\max}\}}{argmax}\ (p^T \cdot f(x, \delta_e)) \\
\quad elseif\ \left(\frac{\partial^2 H(x,p)}{\partial {\delta_e}^2}\Big|_{\delta_{ez2}} < 0 \right) \\
\quad\quad \delta_e{}^* = \underset{\{\delta_{ez2}, \delta_{\min}, \delta_{\max}\}}{argmax}\ (p^T \cdot f(x, \delta_e)) \\
\quad else \\
\quad\quad \delta_e{}^* = \underset{\{\delta_{ez1}, \delta_{ez2}, \delta_{\min}, \delta_{\max}\}}{argmax}\ (p^T \cdot f(x, \delta_e)) \\
\quad endif \\
endif
\end{array}
$$

B. Safe Set Results

The safe set boundary is specified by the zero level set of the scalar valued function $\mathcal{S}(v, \gamma, q, \alpha)$. One way to visualize this four dimensional flight safe set is as a linear array of three dimensional surfaces formed by taking slices along constant values of an independent dimension. Figure 5 illustrates a four dimensional safe set as a sequence of three dimensional surfaces for constant angles of attack values, $S(v, \gamma, q)(\alpha_{const})$ for an unimpaired and impaired aircraft. Figure 6 shows $S(v, \gamma, \alpha)(q = 0)$ corresponding to trim states for straight, wings level flight with the set of viable trim points on the interior. Note both the safe set and the equilibrium point structure is significantly altered in the presence of failures and will severely limit the manner in which the aircraft can be safely maneuvered to remain within the prescribed envelope limits.

V. Conclusions

Ordinarily, for unimpaired aircraft, stall occurs outside of the prescribed flight envelope, therefore envelope protection is an important technology in the prevention of LOC. In this paper we showed the impact of control constraints, including those induced by actuator impairment, on the ability to maneuver within and prevent departure from the flight envelope for the longitudinal dynamics of NASA's GTM. We examined maneuverability by identifying attainable steady motions within the flight envelope and illustrated how the set of viable trim points can change when an actuator impairment occurs. We derive a Hamiltonian for the longitudinal dynamics of GTM which yields an expression for the optimal safety based thrust and elevator control. We then utilize this expression in a level set method framework to solve a partial differential equation to compute safe sets for an unimpaired and impaired elevator.

References

[1] H. Ranter, "Airliner accident statistics 2006," Aviation Safety Network, Tech. Rep., 2007.

[2] J. E. Wilborn and J. V. Foster, "Defining commercial aircraft loss-of-control: a quantitative approach," in *AIAA Atmospheric Flight mechanics Conference and Exhibit*. Providence, Rhode Island: AIAA, 16-19 August 2004.

[3] A. A. Lambregts, G. Nesemeier, J. E. Wilborn, and R. E. Newman, "Airplane upsets: Old problem, new issues," in *AIAA Modeling and Simulation Technologies Conference and Exhibit*. Honolulu, Hawaii: AIAA, 2008.

[4] H. G. Kwatny, J.-E. T. Dongmo, B. C. Chang, G. Bajpai, M. Yasar, and C. Belcastro, "Aircraft accident prevention: Loss-of-control analysis," in *AIAA Guidance, Navigation and Control Conference*, Chicago, 10-13 August 2009.

[5] H. G. Kwatny, J.-E. T. Dongmo, R. C. Allen, B. C. Chang, and G. Bajpai, "Loss-of-control: Perspectives on flight dynamics and control of impaired aircraft," in *AIAA Guidance, Navigation and Control Conference*, Toronto, 2-5 August 2010.

[6] H. G. Kwatny, W. H. Bennett, and J. M. Berg, "Regulation of relaxed stability aircraft," *IEEE Transactions on Automatic Control*, vol. AC-36, no. 11, pp. 1325–1323, 1991.

[7] K. N. Hossain, V. Sharma, M. B. Bragg, and P. G. Voulgaris, "Envelope protection and control adaptation in icing encounters," in *41st AIAA Aerospace Sciences Meeting and Exhibit*, Reno, Nevada, 6-9 January 2003.

[8] S. Unnikrishnan and J. V. R. Prasad, "Carefree handling using reactionary envelope protection method," in *AIAA Guidance, Navigation and Control Conference and Exhibit*, Keystone, CO, 21-24 August 2006.

[9] K. H. Well, "Aircraft control laws for envelope protection," in *AIAA Guidance, Navigation and Control Conference*, Keystone, Colorado, 21-24 August 2006.

[10] M. Oishi, I. M. Mitchell, C. Tomlin, and P. Saint-Pierre, "Computing viable sets and reachable sets to design feedback linearizing control laws under saturation," in

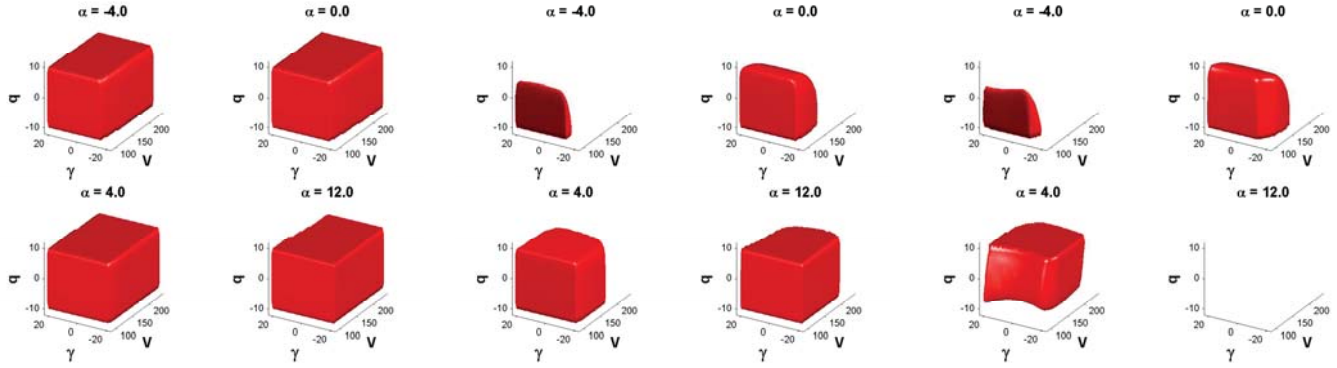

(a) Unimpaired (b) Restricted Elevator (c) Jammed Elevator

Fig. 5. The figure shows the four dimensional safe sets for slices of constant α=(-4,0,4,12) for an unimpaired and two levels of elevator impairment. The figure on the left shows the safe set for the unimpaired aircraft in which case the elevator position ranges from -40 deg to +20 deg. In the center figure, the elevator motion is restricted in the positive direction to + 3 deg, and in the rightmost figure the elevator is stuck at + 3 deg.

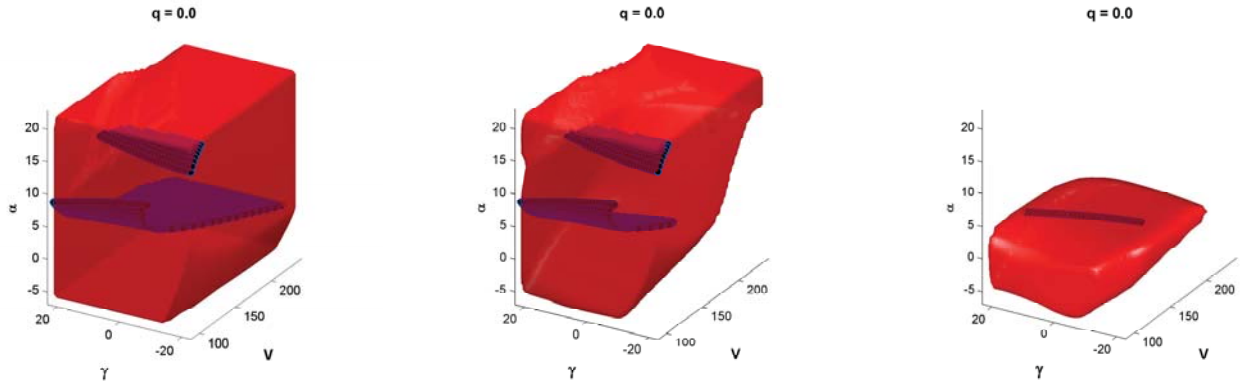

(a) Unimpaired (b) Restricted Elevator (c) Jammed Elevator

Fig. 6. The figure shows the four dimensional safe sets at a slice of q=0 (equilibrium condition) for an unimpaired and two levels of elevator impairment. Attainable equilibrium points for steady (V,γ) are shown in the interior of the safe set. Preventing envelope departure could be difficult for trim points near the safe set boundary.

45th IEEE Conference on Decision and Control. San Diego: IEEE, 2006, pp. 3801–3807.

[11] J. Lygeros, "On reachability and minimum cost optimal control," *Automatica*, vol. 40, pp. 917–927, 2004.

[12] A. Feuer and M. Heymann, "ω-invariance in control systems wiyh bounded controls," *Journal of mathematical Analysis and Applications*, vol. 53, pp. 26–276, 1976.

[13] J. Errico. (2006) http://www.mathworks.com/matlabcentral/fileexchange/8277-fminsearchbnd.

[14] J. Berg and H. G. Kwatny, "An upper bound on the structurally stable regulation of a parameterized family of nonlinear control systems," *Systems and Control Letters*, vol. 23, pp. 85–95, 1994.

[15] ——, "A canonical parameterization of the kronecker form of a matrix pencil," *Automatica*, vol. 31, no. 5, pp. 669–680, 1995.

[16] J. M. Berg and H. G. Kwatny, "Unfolding the zero structure of a linear control system," *Linear Algebra and its Applications*, vol. 235, pp. 19–39, 1997.

[17] B. Stevens and F. Lewis, *Aircraft Control and Simulation*. Wiley, 2003.

[18] J. Lygeros, C. Tomlin, and S. Sastry, "Controllers for reachability specifications for hybrid systems," *Automatica*, vol. 35, no. 3, pp. 349–370, 1999.

[19] I. M. Mitchell, A. M. Bayen, and C. J. Tomlin, "A time-dependent hamilton-jacobi formulation of reachable sets for continuous dynamic games," vol. 50, no. 7, pp. 947–957, 2005.

[20] S. Osher and R. Fedkiw, *Level et Methods and Dynamic Implicit Surfaces*. Springer, 2003.